

**MELT DERIVED FABRICATION OF BIOACTIVE
GLASS AND BIOCOMPATIBILITY
EVALUATION TOWARDS DENTAL PULP STEM
CELL**

NURUL SHAZWANI BINTI MOHD ZAIN

UNIVERSITI SAINS MALAYSIA

2018

**MELT DERIVED FABRICATION OF BIOACTIVE
GLASS AND BIOCOMPATIBILITY
EVALUATION TOWARDS DENTAL PULP STEM
CELL**

by

NURUL SHAZWANI BINTI MOHD ZAIN

**Thesis submitted in fulfilment of the requirements
for the Degree of
Master of Science**

August 2018

ACKNOWLEDGEMENT

First and foremost, I thank Allah SWT for permitting me with health, patience, knowledge, wisdom and strength to complete this work. The journey was priceless and I have learnt from many ways.

A special thanks to Ministry of Higher Education, Malaysia (MyBrain15) and Yayasan Pelajaran Johor (Tabung Pendidikan Sarjana PDT) for the funding scholarship scheme. I would like to thank Universiti Sains Malaysia who provides Research University (RU) grant (1001/CIPPT/814258) in supporting the funding of my research work. I would like to express my sincere gratitude to my main supervisor Associate Professor Dr. Siti Noor Fazliah Mohd Noor and co-supervisor Associate Professor Dr. Hasmaliza Mohamad for their guidance, enthusiasm and continuous support throughout this research and in writing the thesis. Their expertise in numerous areas of the research process has facilitated the advancement of my knowledge and skills.

Furthermore, I would like to thank all of the staff from Craniofacial & Biomaterial Sciences, staffs at Advanced Medical and Dental Institute, Universiti Sains Malaysia and also School of Materials and Mineral Resources Engineering at Engineering Campus, Universiti Sains Malaysia for all their hard work in assisting me towards completing this research. Finally, I would like to express my sincere gratitude to my family especially my mother which has been invaluable. Her ongoing encouragement of my study is what keeps me going on a day-to-day basis. Not to mention my friends and colleagues, Nurul Farhana Ibrahim, Siti Sarah Muhammad Takudin, Siti Nur Liyana Ramlee and also Nik Syahirah Aliaa Nik Sharifulden whom helping me in many ways.

TABLE OF CONTENTS

ACKNOWLEDGEMENT	ii
TABLE OF CONTENTS	iii
LIST OF TABLES	viii
LIST OF FIGURES	ix
LIST OF ABBREVIATIONS	xv
LIST OF SYMBOLS	xviii
ABSTRAK	xix
ABSTRACT	xxi
CHAPTER 1 – INTRODUCTION	1
1.1 Bioglass as biomaterial	1
1.2 Problem statement	2
1.3 Objectives of the project	5
1.4 Research questions	5
1.5 Research hypothesis	6
1.6 Research approaches	6
CHAPTER 2 – LITERATURE REVIEW	9
2.1 Bioactive materials	9
2.2 Bioactive glass	9
2.2.1 Properties of bioactive glass	10
2.2.2 Synthesis of bioactive glass	15
2.2.2(a) Melt quench route	16
2.2.2(b) Sol-gel route	17
2.2.2(c) Melt anneal route	18

2.2.3	Hydroxyl carbonate apatite (HCA) mechanism	19
2.3	Modification in properties and composition of bioactive glass	21
2.3.1	Modifying the properties and composition of original bioactive glass	25
2.3.2	Addition of other element within the bioactive glass composition	28
2.4	Stem cell from the tooth	30
2.4.1	Dental pulp stem cell (DPSC)	31
2.4.2	Stem cells from human exfoliated deciduous tooth (SHED)	33
2.4.3	Stem cells from apical papilla (SCAP)	34
2.4.4	Dental follicle stem cells (DFSC)	35
2.5	Application of bioactive glass in dentistry	36
2.5.1	Filler materials in glass ionomer cements (GIC)	38
2.5.2	Application in root canal therapy	39
2.5.3	Application for pit and fissure sealants	40
2.5.4	Bioactive glass paste	42
2.5.5	Bioactive glass in dental composite	44
CHAPTER 3 – MATERIALS AND METHODS		46
3.1	Fabrication of bioactive glass	46
3.1.1	Materials	46
3.1.1(a)	Silicon Dioxide, SiO ₂	46
3.1.1(b)	Calcium Carbonate, CaCO ₃	46
3.1.1(c)	Sodium Carbonate, Na ₂ CO ₃	47
3.1.1(d)	Phosphorus Pentoxide, P ₂ O ₅	47
3.2	Sample preparation	47
3.2.1	Batching	49
3.2.2	Mixing	50

3.2.3	Melting	50
3.2.4	Quenching	50
3.2.5	Milling and sieving	51
3.3	Maintenance of cell culture	51
3.3.1	DPSC cell lines	51
3.3.2	Thawing frozen cells	52
3.3.3	Cell counting and evaluation of viable cell	52
3.3.4	Passaging confluence cells	53
3.3.5	Cryopreservation	54
3.3.6	Bioactive glass conditioned medium preparation	55
3.3.7	Osteogenic medium preparation	55
3.4	Characterisations and biocompatibility assessment	56
3.4.1	Thermogravimetric analysis (TGA) and differential scanning calorimetry (DSC)	57
3.4.2	Particle size analysis	57
3.4.3	X-Ray Diffraction (XRD) analysis	58
3.4.4	X-Ray Fluorescence (XRF) analysis	58
3.4.5	In vitro bioactivity tests	59
3.4.6	Fourier Transform Infrared (FTIR) spectroscopy	59
3.4.7	pH evaluation	60
3.4.8	Field Emission Scanning Electron Microscope (FESEM)	60
3.4.9	Energy Dispersive X-ray Spectroscopy (EDX)	60
3.4.10	Ion dissolution from bioactive glass in SBF and culture media	61
3.4.11	Inductively Coupled Plasma – Optical Emission Spectrometer (ICP–OES)	61
3.4.12	Alamar Blue assay	62
3.4.13	MTT Assay	63

3.4.14	Alkaline phosphatase (ALP) activity	63
3.4.15	Total DNA assay	64
3.4.16	Alizarin red staining	65
3.4.17	Von kossa staining	65
3.5	Stastical analysis	66
 CHAPTER 4 – RESULTS AND DISCUSSION		67
4.1	Introduction	67
4.2	Fabrication and characterisation of bioactive glasses via melt derived method	68
4.2.1	Thermal analysis of bioactive glass	68
4.2.1(a)	Thermal analysis of bioactive glass 45S5	68
4.2.1(b)	Thermal analysis of bioactive glass 44S	70
4.2.2	Particle size analysis	72
4.2.3	X-Ray Fluorescence (XRF) Analysis	74
4.2.4	X-Ray Diffraction (XRD) Analysis	77
4.2.5	Fourier transform infrared (FTIR) spectroscopy	78
4.3	Characterisation of physical properties for bioactive glasses by using in vitro bioactivity tests	81
4.3.1	Fourier transforms infrared spectroscope (FTIR) analysis	81
4.3.2	Field Emission Scanning Electron Microscope (FESEM) and Energy Dispersive X-ray Spectroscopy (EDX) analysis	87
4.3.3	Inductively Coupled Plasma – Optical Emission Spectrometry (ICP – OES) analysis	95
4.3.4	pH evaluation	102
4.4	Assessment of biocompatibility of melt derived bioactive glasses towards dental pulp stem cells (DPSC)	107
4.4.1	Alamar Blue (AB) assay	107
4.4.2	MTT assay	112

4.5	Assessment of osteoinduction properties of melt derived bioactive glasses towards dental pulp stem cells (DPSC)	117
4.5.1	MTT assay	117
4.5.2	ALP activity and total DNA quantification	120
4.5.3	Alizarin red staining	126
4.5.4	Von kossa staining	135
CHAPTER 5 – CONCLUSION AND RECOMMENDATIONS		145
5.1	Conclusion	145
5.2	Limitation of this research	147
5.3	Recommendation for future research	147
REFERENCES		148
APPENDICES		
LIST OF PUBLICATION		

LIST OF TABLES

	Page
Table 2.1 Properties of bioactive glasses. Adapted from Jones and Clare (2012).	11
Table 2.2 Flexural strength, microhardness, compressive strength and density of bioactive glasses. Adapted from Jones and Clare (2012); Vyas, et al. (2015); Vyas et al. (2016).	11
Table 2.3 Modification in bioactive glass composition based on standard 45S5 Bioglass [®] .	22
Table 2.4 Application of bioactive glass powder in dentistry.	37
Table 3.1 The bioactive glass composition used in this project.	49
Table 3.2 Composition of normal medium (NM) and osteogenic medium (OM).	56
Table 3.3 Emission lines used for the ICP-OES measurements.	62
Table 4.1 Particle size distribution of bioactive glass 45S5 and 44S.	73
Table 4.2 XRF result for bioactive glass 45S5 and 44S.	74
Table 4.3 Functional groups exist in bioactive glass 45S5 and 44S.	79
Table 4.4 Functional groups in bioactive glass 45S5 upon immersion in SBF solution.	82
Table 4.5 Functional groups in bioactive glass 44S upon immersion in SBF solution.	85

LIST OF FIGURES

		Page
Figure 1.1	The flow chart of the experimental procedure.	8
Figure 2.1	The biological responses to ionic dissolution products of bioactive glasses. Adapted from Hoppe et al., (2011).	14
Figure 2.2	Methods for analysing the cellular response to degradable biomaterials. Adapted from Hoppe et al., (2011).	15
Figure 2.3	Compositional diagrams for bone-bonding in weight percentage. Adapted from Hench (2006).	21
Figure 2.4	Stem cells that can be obtained from the oral and maxillofacial region. Adapted from Egusa et al., (2012).	31
Figure 3.1	Fabrication of bioactive glass.	48
Figure 3.2	The melting profile of the bioactive glass.	50
Figure 3.3	Heat treatment profile for the TGA/DSC.	57
Figure 4.1	TGA trend for raw materials of bioactive glass 45S5 powder heated until 1200 °C.	69
Figure 4.2	DSC trend for raw materials of bioactive glass 45S5 powder heated until 1200 °C. The ↓ represents endothermic reaction occurring at 740 °C, 860 °C and ↑ represents exothermic reaction occurring at 870 °C.	69
Figure 4.3	TGA trend for raw materials of bioactive glass 44S powder heated until 1200 °C.	70
Figure 4.4	DSC for raw materials of bioactive glass 44S powder heated until 1200 °C. The ↓ represents endothermic reaction occurring at 703 °C, 830 °C and ↑ represents exothermic reaction occurring at 865 °C.	71
Figure 4.5	Particle size distribution of bioactive glass 45S5 and 44S.	72
Figure 4.6	XRD analysis for bioactive glass 45S5 and 44S.	77
Figure 4.7	FTIR analysis for bioactive glass 45S5 and 44S.	78
Figure 4.8	FTIR analysis for bioactive glass 45S5 upon immersion in SBF solution.	82
Figure 4.9	FTIR analysis for bioactive glass 44S upon immersion in SBF solution.	84

Figure 4.10	The SEM images and EDX analysis for BG 45S5 powder before (a1-a2) and after immersion in SBF solution for day 1 (b1-b2), day 7 (c1-c2) and day 21 (d1-d2). EDX analysis was based on the marked area (X) shown in red. HA (yellow) and HCA (green) exist based on the marked area (X).	88
Figure 4.11	The SEM images and EDX analysis for BG 44S powder before (a1-a2) and after immersion in SBF solution for day 1 (b1-b2), day 7 (c1-c2) and day 21 (d1-d2). EDX analysis was based on the marked area (X) shown in red. HA (yellow) and HCA (green) exist based on the marked area (X).	91
Figure 4.12	Ion dissolution profiles released from bioactive glass 45S5 and 44S in SBF solution for (a) Si, (b) Na, (c) Ca and (d) P.	96
Figure 4.13	Ion dissolution profiles released from bioactive glass 45S5 and 44S in DMEM culture media for (a) Si, (b) Na, (c) Ca and (d) P.	100
Figure 4.14	pH behaviour of SBF solution upon immersion of bioactive glass 45S5 and 44S.	103
Figure 4.15	pH behaviour of DMEM solution after immersion of bioactive glass 45S5 and 44S.	105
Figure 4.16	The DPSC cell viability upon exposure to BG-conditioned medium containing (a) BG 45S5 and (b) BG 44S as assessed using Alamar Blue (AB) assay. * denotes significant of the marked bar compared to DPSC incubated with control medium at the same time point. + denotes significant of the marked bar compared to DPSC incubated with 1.0 mg/ml BG-conditioned media at the same time point.	108
Figure 4.17	The DPSC cell viability upon exposure to BG-conditioned medium containing (a) BG 45S5 and (b) BG 44S compared to control.	111
Figure 4.18	The DPSC proliferative activity towards BG-conditioned medium containing (a) BG 45S5 and (b) BG 44S as assessed using MTT Assay. * denotes a significant of the marked bar compared to DPSC incubated with control medium at the same time point.	113
Figure 4.19	The DPSC cell proliferation upon exposure to BG-conditioned medium containing (a) BG 45S5 and (b) BG 44S compared to control.	116

Figure 4.20	DPSC proliferative activity in NM and OM containing (a) BG 45S5 and (b) BG 44S as assessed using MTT Assay. * denotes a significant of the marked bar compared to DPSC incubated with control at the same time point.	118
Figure 4.21	The ALP activity of DPSC cultured in NM and OM containing (a) 45S5 and (b) 44S BG-conditioned medium normalised to total DNA content from the same cell lysates. * denotes a significant of the marked bar compared to DPSC incubated with control at the same time point.	121
Figure 4.22	The ALP activity of DPSC cultured in NM and OM containing (a) 45S5 and (b) 44S BG-conditioned medium. * denotes a significant of the marked bar compared to DPSC incubated with control at the same time point.	123
Figure 4.23	The DNA assay as a representative of the total number of DPSC cultured in NM and OM containing (a) 45S5 and (b) 44S BG-conditioned medium. * denotes a significant of the marked bar compared to DPSC incubated with control at the same time point.	124
Figure 4.24	DPSC upon exposure to NM control using Alizarin red staining at days 14 and 21. Alizarin red staining detects calcium deposit in DPSC as shown by the arrow (black). Scale bar is 200 μm .	127
Figure 4.25	DPSC upon exposure to 2.0 mg/ml NM 45S5 BG-conditioned medium using Alizarin red staining at days 14 and 21. Alizarin red staining detects calcium deposit in DPSC as shown by the arrow (black). Scale bar is 200 μm .	127
Figure 4.26	DPSC upon exposure to 4.0 mg/ml NM 45S5 BG-conditioned medium using Alizarin red staining at days 14 and 21. Alizarin red staining detects calcium deposit in DPSC as shown by the arrow (black). Scale bar is 200 μm .	128
Figure 4.27	DPSC upon exposure to OM control using Alizarin red staining at days 14 and 21. Alizarin red staining detects calcium deposit in DPSC as shown by the arrow (black). Scale bar is 200 μm .	128

Figure 4.28	DPSC upon exposure to 2.0 mg/ml OM 45S5 BG-conditioned medium using Alizarin red staining at days 14 and 21. Alizarin red staining detects calcium deposit in DPSC as shown by the arrow (black). Scale bar is 200 μ m.	129
Figure 4.29	DPSC upon exposure to 4.0 mg/ml OM 45S5 BG-conditioned medium using Alizarin red staining at days 14 and 21. Alizarin red staining detects calcium deposit in DPSC as shown by the arrow (black). Scale bar is 200 μ m.	129
Figure 4.30	DPSC upon exposure to NM control using Alizarin red staining at days 14 and 21. Alizarin red staining detects calcium deposit in DPSC as shown by the arrow (black). Scale bar is 200 μ m.	130
Figure 4.31	DPSC upon exposure 2.0 mg/ml NM 44S BG-conditioned medium using Alizarin red staining at days 14 and 21. Alizarin red staining detects calcium deposit in DPSC as shown by the arrow (black). Scale bar is 200 μ m.	130
Figure 4.32	DPSC upon exposure to 4.0 mg/ml NM 44S BG-conditioned medium using Alizarin red staining at days 14 and 21. Alizarin red staining detects calcium deposit in DPSC as shown by the arrow (black). Scale bar is 200 μ m.	131
Figure 4.33	DPSC upon exposure to OM control using Alizarin red staining at days 14 and 21. Alizarin red staining detects calcium deposit in DPSC as shown by the arrow (black). Scale bar is 200 μ m.	131
Figure 4.34	DPSC upon exposure to 2.0 mg/ml OM 44S BG-conditioned medium using Alizarin red staining at days 14 and 21. Alizarin red staining detects calcium deposit in DPSC as shown by the arrow (black). Scale bar is 200 μ m.	132
Figure 4.35	DPSC upon exposure to 4.0 mg/ml OM 44S BG-conditioned medium using Alizarin red staining at days 14 and 21. Alizarin red staining detects calcium deposit in DPSC as shown by the arrow (black). Scale bar is 200 μ m.	132

Figure 4.36	DPSC upon exposure to NM control using von kossa staining at days 14 and 21. Von kossa staining detects mineralised nodule, calcium phosphate as black stain in DPSC as shown by the arrow (black). Scale bar is 200 μ m.	135
Figure 4.37	DPSC upon exposure to 2.0 mg/ml NM 45S5 BG-conditioned medium using von kossa staining at days 14 and 21. Von kossa staining detects mineralised nodule, calcium phosphate as black stain in DPSC as shown by the arrow (black). Scale bar is 200 μ m.	136
Figure 4.38	DPSC upon exposure to 4.0 mg/ml NM 45S5 BG-conditioned medium using von kossa staining at days 14 and 21. Von kossa staining detects mineralised nodule, calcium phosphate as black stain in DPSC as shown by the arrow (black). Scale bar is 200 μ m.	136
Figure 4.39	DPSC upon exposure to OM control using von kossa staining at days 14 and 21. Von kossa staining detects mineralised nodule, calcium phosphate as black stain in DPSC as shown by the arrow (black). Scale bar is 200 μ m.	137
Figure 4.40	DPSC upon exposure to 2.0 mg/ml OM 45S5 BG-conditioned medium using von kossa staining at days 14 and 21. Von kossa staining detects mineralised nodule, calcium phosphate as black stain in DPSC as shown by the arrow (black). Scale bar is 200 μ m.	137
Figure 4.41	DPSC upon exposure to 4.0 mg/ml OM 45S5 BG-conditioned medium using von kossa staining at days 14 and 21. Von kossa staining detects mineralised nodule, calcium phosphate as black stain in DPSC as shown by the arrow (black). Scale bar is 200 μ m.	138
Figure 4.42	DPSC upon exposure to NM control using von kossa staining at days 14 and 21. Von kossa staining detects mineralised nodule, calcium phosphate as black stain in DPSC as shown by the arrow (black). Scale bar is 200 μ m.	138
Figure 4.43	DPSC upon exposure to 2.0 mg/ml NM 44S BG-conditioned medium using von kossa staining at days 14 and 21. Von kossa staining detects mineralised nodule, calcium phosphate as black stain in DPSC as shown by the arrow (black). Scale bar is 200 μ m.	139

Figure 4.44	DPSC upon exposure to 4.0 mg/ml NM 44S BG-conditioned medium using von kossa staining at days 14 and 21. Von kossa staining detects mineralised nodule, calcium phosphate as black stain in DPSC as shown by the arrow (black). Scale bar is 200 μ m.	139
Figure 4.45	DPSC upon exposure to OM control using von kossa staining at days 14 and 21. Von kossa staining detects mineralised nodule, calcium phosphate as black stain in DPSC as shown by the arrow (black). Scale bar is 200 μ m.	140
Figure 4.46	DPSC upon exposure to 2.0 mg/ml OM 44S BG-conditioned medium using von kossa staining at days 14 and 21. Von kossa staining detects mineralised nodule, calcium phosphate as black stain in DPSC as shown by the arrow (black). Scale bar is 200 μ m.	140
Figure 4.47	DPSC upon exposure to 4.0 mg/ml OM 44S BG-conditioned medium using von kossa staining at days 14 and 21. Von kossa staining detects mineralised nodule, calcium phosphate as black stain in DPSC as shown by the arrow (black). Scale bar is 200 μ m.	141

LIST OF ABBREVIATIONS

AB	Alamar blue
ALP	Alkaline phosphatase
BG	Bioactive glass
BGN	Bioactive glass nanoparticles
BMSC	Bone marrow stromal cells
BO	Bridging oxygen
DFSC	Dental follicle stem cells
DMEM	Dulbecco's modified eagle medium
DMSO	Dimethyl sulfoxide
DOE	Design of experiment
DPBS	Dulbecco's phosphate buffered saline
DPSC	Dental pulp stem cells
DSC	Differential scanning calorimetry
ECM	Extracellular matrix mineralisation
EDX	Energy dispersive x-ray spectroscopy
FESEM	Field emission scanning electron microscope
FTIR	Fourier transform infrared spectroscopy
GIC	Glass ionomer cement
GP	Gutta pecha

HA	Hydroxyapatite
HCA	Hydroxyl carbonate apatite
ICP-OES	Inductively coupled plasma-optical emission spectroscopy
MTA	Mineral trioxide aggregate
MTT	Methylthiazolyldiphenyl-tetrazolium bromide
NBO	Non-bridging oxygen
Nc	Network connectivity
NM	Normal medium
OM	Osteogenic medium
PBS	Phosphate buffered saline
PDLSC	Periodontal ligament stem cells
PSA	Particle size analysis
rpm	Revolutions per minute
TGA	Thermogravimetric analysis
T _c	Crystallization temperature
T _g	Glass transition temperature
T _m	Melting temperature
TGPC	Tooth germ progenitor cells
SBF	Simulated body fluid
SCAP	Stem cells from apical papilla

SGCS	Salivary gland-derived stem cells
SHED	Stem cells from human exfoliated deciduous teeth
v/v	Volume per volume
WHO	World health organisation
w/v	Weight per volume
XRD	X-ray diffraction
XRF	X-ray fluorescence

LIST OF SYMBOLS

a.u	Arbitrary unit
°	Degree
°C	Degree celcius
g	Gram
GPa	Giga pascal
g/mol	Gram per mole
θ	Incidence Angle Of X-Ray Beam
MPa	Mega pascal
μm	Micrometer
μM	Micromolar
mol.%	Mole percentages
Nm	Nanometer
%	Percentage
wt.%	Weight percentages

**PENGHASILAN KACA AKTIF BIO BERASASKAN PELEBURAN DAN
PENILAIAN KEBOLEHSERASIAN BIO TERHADAP SEL INDUK PULPA
GIGI**

ABSTRAK

Kaca aktif bio berupaya untuk melekap dan membentuk tisu keras dan tisu lembut, seterusnya menggalakkan pertumbuhan tulang. Kaca aktif bio 45S5 dengan komposisi 46.1% SiO₂, 26.9% CaO, 24.4% Na₂O dan 2.5% P₂O₅ dalam peratusan mol (mol.%) dan satu komposisi baru (BG 44S) dengan jaringan kesambungan yang sama telah dihasilkan menggunakan kaedah peleburan pada suhu dan tempoh rendaman yang sama. Komposisi 44S dicadangkan untuk menurunkan suhu peleburan ketika penghasilan. Penyediaan kaca aktif bio merangkumi proses pengelompokan, pencampuran, peleburan pada 1400 °C, lindap-kejut air, pengisaran dan pengayakan. Kaca aktif bio 45S5 mempunyai purata saiz zarah lebih rendah (11.8 µm) berdasarkan analisis saiz zarah. Kedua-dua kaca aktif bio berada di dalam fasa amorf berdasarkan analisis pembelauan sinar-X (XRD) dan mempunyai kebanyakannya jaringan silikat berdasarkan kehadiran kumpulan berfungsi Si-O-Si menurut Spektroskopi Inframerah Transformasi Fourier. Kedua-dua jenis kaca aktif bio ini menjalani pengeraman di dalam cecair badan tiruan (SBF) untuk menilai tahap bioaktiviti untuk pembentukan lapisan hidroksi karbonat apatit (HCA) yang diikuti dengan pencirian. Kumpulan berfungsi bagi ikatan P-O dan C-O wujud pada hari pertama bagi kaca aktif bio 44S, manakala wujud pada hari ketujuh bagi kaca aktif bio 45S5, yang dikaitkan dengan pembentukan lapisan HCA. Pembentukan lapisan hidroksiapatit (HA) di atas kedua-dua permukaan kaca aktif bio bermula pada

hari pertama, diikuti dengan pembentukan kelompok kristal HCA pada hari 21 berdasarkan imej mikroskop pengimbas elektron dan analisis spektroskopi serakan tenaga sinar-X (EDX) selepas direndam di dalam cecair SBF. Pembebasan ion daripada kedua-dua kaca aktif bio, terutamanya ion kalsium dan fosforus di dalam cecair SBF dan Medium Eagle Terubahsuai oleh Dulbecco (DMEM) berdasarkan spektrometer pemancaran optik - plasma terganggu beraruhan (ICP-OES) menunjukkan bahawa pembentukan HCA berlaku pada kedua-dua kaca aktif bio yang berkait rapat dengan peningkatan nilai pH selepas melalui pengeraman selama 240 minit. Sel induk pulpa gigi (DPSC) menunjukkan kelangsungan sel yang lebih tinggi di dalam cerakin Alamar Blue (AB) dan perkembangbiakan sel yang lebih tinggi dalam cerakin metiltiazolildifenil-tetrazolium bromida (MTT) apabila terdedah kepada nisbah serbuk kaca aktif bio kepada cecair yang lebih rendah (1 – 2 mg/ml) untuk kedua-dua media yang mengandungi BG yang menunjukkan biokeserasian terhadap DPSC. Pendedahan DPSC kepada media yang mengandungi nisbah serbuk BG kepada cecair yang lebih rendah (1 – 2 mg/ml) bagi kedua-dua kaca aktif bio 45S5 dan 44S tanpa agen induktif osteogenik menunjukkan sifat induksi osteogenik berdasarkan ujian MTT, aktiviti fosfatase beralkali (ALP) dan cerakin jumlah DNA. DPSC yang terdedah kepada medium yang mengandungi agen induktif osteogenik menunjukkan pemineralan berlebihan berdasarkan pewarnaan von Kossa dan Alizarin merah. Media yang mengandungi kaca aktif bio 45S5 dan 44S merangsang sifat osteogenik dalam DPSC. Kesimpulannya, kaca aktif bio 45S5 dan 44S berjaya dihasilkan dan keduanya adalah bioserasi terhadap DPSC hingga meningkatkan kelangsungan, perkembangbiakan dan pembezaan osteogenik. Oleh itu, kaca aktif bio ini menunjukkan potensi untuk aplikasi dalam pergigian regeneratif.

**MELT DERIVED FABRICATION OF BIOACTIVE GLASS AND
BIOCOMPATIBILITY EVALUATION TOWARDS DENTAL PULP STEM
CELL**

ABSTRACT

Bioactive glass (BG) has the ability to bond to hard and soft tissues, and promotes bone growth. BG 45S5, with composition of 46.1% SiO₂, 26.9% CaO, 24.4% Na₂O, and 2.5% P₂O₅ in mole percentages (mol.%), and a new composition (BG 44S), with similar network connectivity were fabricated *via* melt derived route using similar melting temperature and soaking time. The 44S composition was proposed to decrease melting temperature during fabrication. The BG preparations included batching, mixing, melting at 1400 °C, water quenching, milling, and sieving. BG 45S5 possessed lower average particle size (11.8 µm) based on the particle size analysis. Both BG were in amorphous phase based on X-Ray Diffraction (XRD) analyses and contained mainly silicate network, with Si-O-Si functional groups, using Fourier Transform Infrared spectroscopy. Both BG were subjected to simulated body fluid incubation to assess the bioactivity for hydroxyl carbonate apatite (HCA) layer formation, followed by characterisations. Functional groups of P-O and C-O bonds, which attributed to HCA layer formation were present at day 1 for BG 44S, and at day 7 for BG 45S5. The hydroxyapatite (HA) layer started to develop on both BG surfaces at day 1, followed by formation of HCA cluster crystal at day 21 based on Scanning Electron Microscope (SEM) images and Energy Dispersive X-ray Spectroscopy (EDX) analyses upon immersion in SBF solution. Ionic release from both BG, especially calcium and phosphorus ions in SBF solution

and Dulbecco's Modified Eagle Medium (DMEM) based on the inductively coupled plasma – optical emission spectrometer showed that HCA formation occurred on both BG surfaces, which corresponded to the increasing pH within 240 minutes incubation. Exposure of dental pulp stem cells (DPSC) to lower BG powder to liquid ratio (1 – 2 mg/ml) for both BG-conditioned media showed higher cell viability in Alamar Blue assay and higher cell proliferation in methylthiazolyldiphenyl-tetrazolium bromide (MTT) assay, highlighting biocompatibility towards DPSC. DPSC exposed to lower BG powder to liquid ratio (1 – 2 mg/ml) for both BG 45S5 and 44S without an osteogenic inductive agent showed osteoinduction properties based on MTT, alkaline phosphatase activity, and total DNA assays. DPSC exposed to medium containing osteogenic inductive agent showed greater mineralisation based on von Kossa and Alizarin red staining. The 45S5 and 44S BG-conditioned media promoted osteogenic properties of DPSC. In conclusion, BG 45S5 and 44S were successfully fabricated and biocompatible towards DPSC, thus enhancing its viability, proliferation, and osteogenic differentiation. Hence, these bioactive glasses showed potential for application in regenerative dentistry.

CHAPTER 1

INTRODUCTION

1.1 Bioglass as biomaterial

Bioactive materials (biomaterial) are materials which can stimulate a biological response at the interface of the materials by forming bonds between the tissues and the material itself. Furthermore, biomaterial are classified into Class A and Class B. Osteopductive material (Class A) is able to produce both an intracellular and extracellular responses at its interface (Cao and Hench, 1996). Bioactive glass (BG) is classified as Class A biomaterial that is able to form bonds with both hard and soft tissues such as bone and teeth. 45S5 Bioglass[®] was the first fabrication of BG by Professor Hench in 1969 which having composition of 46.1% SiO₂, 26.9% CaO, 24.4% Na₂O and 2.5% P₂O₅ in mole percentages (mol.%).

BG can be fabricated in many forms that are suitable for various applications such as powders, rods, disc and also nanoparticles. Two methods commonly used to fabricate BG are through melt derived route (Ibrahim et al., 2017a) and also sol-gel route (Noor et al., 2016b). Melt derived route requires high temperature usually above 1000 °C while sol-gel route usually requires temperature below 1000 °C. However, fabrication of BG requires longer period for sol-gel route compared to melt derived route.

The bioactivity of BG is represented by the formation of hydroxyapatite (HA) and hydroxylcarbonate apatite (HCA) layer on BG surfaces when it is dissolved in simulated body fluids (SBF) (Kokubo and Takadama, 2006). Furthermore, the bioactivity of BG can also be predicted by calculating the network connectivity (Nc) based on its composition especially for melt derived bioactive glass. The 45S5

Bioglass[®] has network connectivity of 2.12 ($N_c = 2.12$). However, the bioactive glasses which had network connectivity (N_c) more than 2.6 are likely to be less bioactive (Jones, 2013; O'Donnell et al., 2008a).

The BG is widely used and being studied especially in dental applications for restorative and endodontic therapy. Recently, the BG has been studied for dental desensitising agent (Ma et al., 2017), dentine mineralisation (Wang et al., 2011b), antibacterial purposes (Liu et al., 2016a) and as inorganic fillers (Alhashimi et al., 2017). Furthermore, the effect of BG towards many cells is studied for biocompatibility (De Caluwé et al., 2017), cell viability, differentiation ability (Houreh et al., 2017), cell proliferation and also osteoinductive purposes (Silva et al., 2017).

Dental pulp stem cells (DPSC) can be obtained from the dental pulp tissue located in the central part of the tooth within the dentin. Furthermore, Gronthos et al., (2002) showed that DPSC possessed high proliferative potential, self-renewal capacities and also multi-lineage differentiation. Tissue engineering requires materials which are biocompatible that can carry signalling molecules and cells that are easily available. Thus, bioactive materials such as BG are needed in tissue engineering due to the ionic dissolution products release from the BG itself which can stimulate cell proliferation and also osteoblast proliferation (Gentleman et al., 2010).

1.2 Problem statement

Common oral diseases causes damaged to teeth and the teeth need to be repaired and treated. It is considered a major health problem when tooth loss happens commonly caused by periodontal disease, trauma and caries (Zhang et al., 2006). Periodontal disease and caries are two major dental diseases which have high prevalence rates

worldwide (Vaithlingam et al., 2017). World Health Organisation (WHO) stated more than 95% adults have caries which often leading to discomfort and pain (World Health Organisation, 2017). For adults in Malaysia, from 1990 until 2000 shows that dental caries is increasing with increasing age (Oral Health Division, 2011). Caries may develop in the crowns and roots of teeth beginning in early childhood. Caries can be treated by dental materials but can cause the tooth to be destroyed without proper care (Selwitz et al., 2007). Caries can be the primary cause for oral pain and also tooth loss. Thus, finding solutions to prevent and also treat dental caries has become critical (Li et al., 2013).

Currently, various dental materials exist for treatment of caries such as mineral trioxide aggregate (MTA) (Flores-Ledesma et al., 2017), amalgam, glass ionomer cement (GIC) (Krämer et al., 2017) and dental composite (Chatzistavrou et al., 2015). There are many developments and tests of dental materials as protective agents for the dentin-pulp complex in dental tissue engineering especially cases involving pulpal exposure or near exposure. Furthermore, biomaterials such as BG are suitable for bone and teeth repair due to the released ionic dissolution products that could promote the cells toward a path of regeneration and also self-repair. Thus, BG is very much needed for dental materials especially for dental pulp tissue regeneration and repair.

Fabrication of BG 45S5 *via* melt derived route required high melting temperature. In the current project, two bioactive glasses were fabricated *via* melt derived route using the same melting temperature with the same soaking time. The fabricated bioactive glasses have the same value of network connectivity (N_c) with the BG 45S5 ($N_c = 2.12$) but with different composition. O'Donnell et al., (2008) discovered

composition of the bioactive glass by substituting P_2O_5 and also fixing the $Na_2O:CaO$ ratio (1.00:0.87). The current project fabricates a new composition of bioactive glass by fixing the $Na_2O:CaO$ ratio (1.00:0.87) and contain similar amount of P_2O_5 with the 45S5 bioactive glass based on Appendix A. Thus, composition of the new BG being modified in order to decrease the melting temperature that is required for fabrication process. Furthermore, new composition of BG has been fabricated at lower melting temperature which helps to reduce the cost during manufacturing process (Ibrahim et al., 2017a).

BG 45S5 being market as NovaBone (NovaBone Products LLC) used for bone regeneration and Novamin[®] (NovaMin Technology, FL) which used for hypersensitivity in Sensodyne Repair and Protect toothpaste (Jones, 2013). Currently, BG 45S5 being added into other dental materials and test towards DPSC. However, limited study is available for BG 45S5 towards DPSC especially for cell culture studies. Thus, characteristic of both bioactive glasses using *in vitro* bioactivity tests and effect of the fabricated bioactive glasses towards DPSC were studied in the current project. Therefore, the fabricated bioactive glasses are investigated as usage for future dental materials.

1.3 Objectives of the project

The general objective of the project is to develop bioactive glasses by using melt derived method and assess its compatibility towards cells. The specific objectives of the project are as listed below:

- i. To fabricate bioactive glasses by using melt derived method.
- ii. To characterise the physical properties of bioactive glasses by using *in vitro* bioactivity tests.
- iii. To assess the biocompatibility of melt derived bioactive glasses towards human dental pulp stem cells (DPSC) using Alamar Blue (AB) and MTT assays.
- iv. To assess the osteoinduction properties of melt derived bioactive glasses towards human dental pulp stem cells (DPSC) using MTT assay, alkaline phosphatase (ALP) activity, total DNA assay, Von Kossa staining and Alizarin red staining.

1.4 Research questions

The research questions of the project are as listed below:

- i. Are both bioactive glasses able to be fabricated by using melt derived method?
- ii. Are the physical properties of both bioactive glasses different after *in vitro* bioactivity tests?
- iii. Are both bioactive glasses biocompatible to DPSC?
- iv. Does DPSC show osteoinduction properties upon exposure towards both bioactive glasses?

1.5 Research hypothesis

The hypotheses of the project are as listed below:

- i. Both bioactive glasses are able to be fabricated by melt derived method.
- ii. Physical properties of both bioactive glasses change after *in vitro* bioactivity tests.
- iii. Both bioactive glasses are biocompatible to DPSC.
- iv. DPSC able to show osteoinduction properties upon exposure towards both bioactive glasses.

1.6 Research approaches

The bioactive glasses that contain SiO₂, CaCO₃, Na₂CO₃ and P₂O₅ as raw materials were fabricated using melt derived method, subjected to characterisation and bioactivity investigations. The BG powders were characterised using thermogravimetric analysis (TGA) and differential scanning calorimetry (DSC), particle size analysis, x-ray diffraction (XRD) analysis, x-ray fluorescence (XRF) and fourier transform infrared (FTIR) spectroscopy. Then, the bioactive glasses were subjected to simulated body fluid (SBF) incubation to assess bioactivity for formation of hydroxyapatite (HA) layer followed by characterisation using fourier transform infrared (FTIR) spectroscopy, pH evaluation, field emission scanning electron microscope (FESEM), energy dispersive x-ray spectroscopy (EDX) and inductively coupled plasma – optical emission spectrometer (ICP–OES).

The biocompatibility of bioactive glasses was assessed using BG-conditioned medium with different powder to liquid ratio (1, 1.5, 2, 4 and 6 mg/ml) towards dental pulp stem cells (DPSC) using Alamar Blue and MTT assays. The osteogenic medium were prepared using BG-conditioned medium with different powder to

liquid ratio (1, 2 and 4 mg/ml) by adding osteogenic inductive agents. Then, the osteogenic medium were exposed toward dental pulp stem cells (DPSC) to assess osteoinduction properties using MTT assay, alkaline phosphatase (ALP) activity, total DNA assay, Von Kossa and Alizarin red stainings. The flow chart of the experimental procedure is shown in Figure 1.1 respectively.

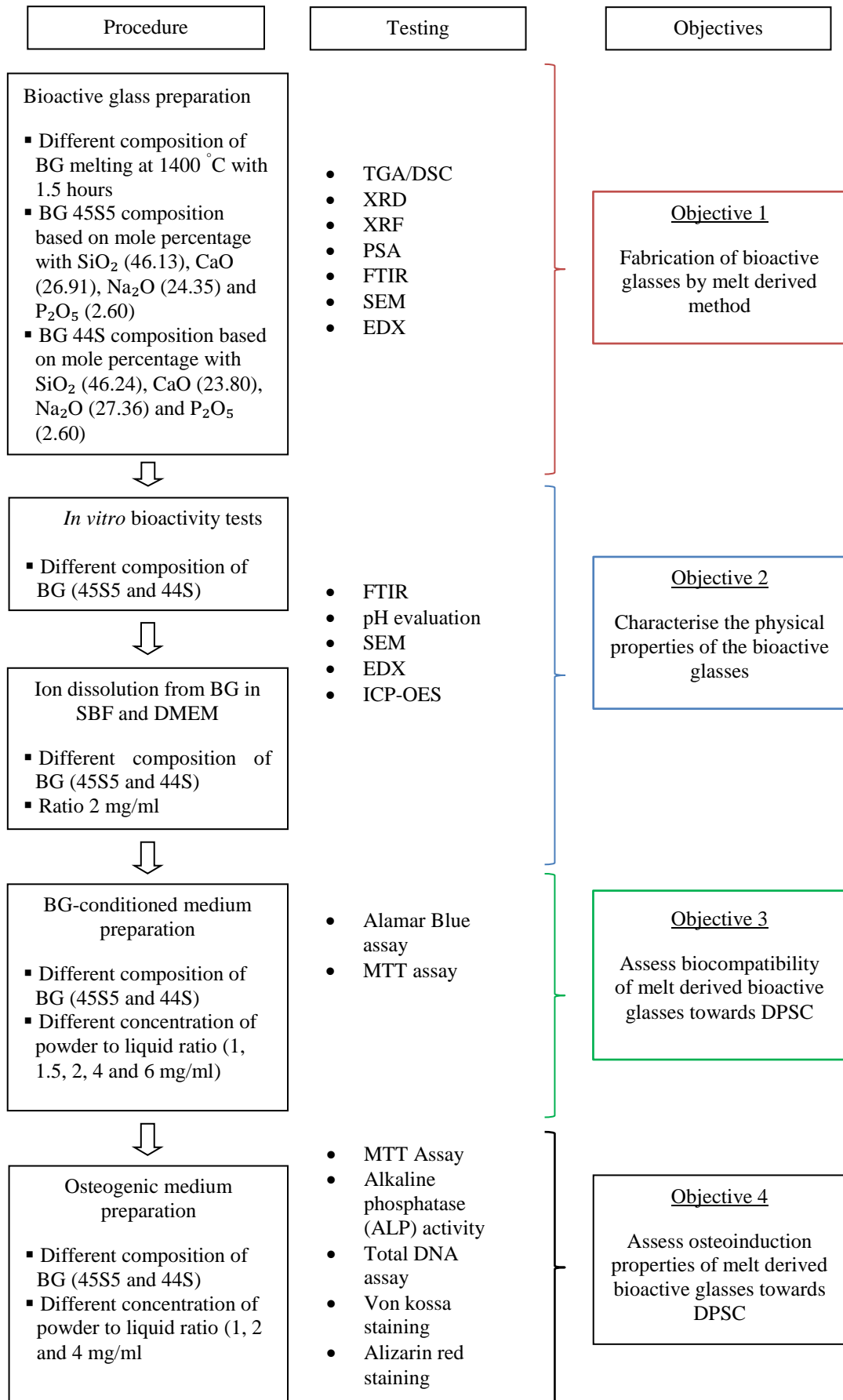


Figure 1.1: The flow chart of the experimental procedure.

CHAPTER 2

LITERATURE REVIEW

2.1 Bioactive materials

The basic function of a biomaterial is to replace damaged or disease tissues (Maçon et al., 2017). Bioactivity reflects the characteristics for a material that is able to create bonding with the host tissues. Bioactive materials is defined as materials that are able to induce specific biological activity at the interface of the material due to the bonding created between the living tissues and the material itself (Polymeris et al., 2017). Currently, biomaterials received extensive researched for commercialisation and used especially for biomedical application. Furthermore, biomaterials were widely used especially in dental applications and medical field.

Bioactive materials include hydroxyapatite (HA) ceramics, bioactive glass, bioactive glass ceramics and also bioactive glass composite. Moreover, bioactive materials were classified into 2 classes which are Class A and Class B (Cao and Hench, 1996). Class A is for osteopductive materials where the materials itself induce an intracellular and an extracellular response at the interface of the materials. Meanwhile, Class B is osteoconductive materials that induce an extracellular response only at the interface of the materials. Bioactive glasses were classified as biomaterials Class A due to the formation of bonding with soft and hard tissues (Cao and Hench, 1996).

2.2 Bioactive glass

Bioactive glass (BG) was discovered as one of the bioactive materials Class A possessing osteoconductive and osteoinductive properties. There were various BG compositions available in the literature. The first fabrication of bioactive glass which

is 45S5 Bioglass[®] was made by Professor Hench in 1969. BG 45S5 contained 46.1% SiO₂, 26.9% CaO, 24.4% Na₂O and 2.5% P₂O₅ in mole percentages (mol.%). BG can be fabricated in various forms such as powders (Zain et al., 2017), disc (Sheng et al., 2016), films (Francis et al., 2016) and also bioceramic scaffolds (Bakopoulou et al., 2016) by using various methods of fabrication such as foam replica, melt derived, sol-gel and isostatic pressing.

Products derived from BG 45S5 include NovaMin[®] (NovaMin[®] Technology, USA) and PerioGlass (NovaBone Osteobiologics, USA) (Deliormanlı, 2017). Both products were commercialised and widely used especially for dental applications. BG differ from any other bioactive materials since they possess certain properties and characteristics. Furthermore, bond formation with bone occurred when hydroxyl apatite (HA) and hydroxyl carbonate apatite (HCA) layer were detected upon BG 45S5 immersion in simulated body fluid (SBF) (Groh et al., 2014).

The ability of a BG to form hydroxyl apatite (HA) layer is often taken as an indication of its bioactivity when the bioactive glass is immersed in the simulated body fluid (SBF). BG is able to regenerate human bone, able to degrade in solution, release ionic dissolution products from the bioactive glass and also form apatite layer in short period of time on the surface of the bioactive glass. Furthermore, the ionic dissolution products from BG can be controlled and tailored for regeneration of tissues (Houreh et al., 2017).

2.2.1 Properties of bioactive glass

Nowadays, researchers investigated and fabricated new BG to improve the properties of BG 45S5 such as thermal, mechanical, physical and chemical. BG 45S5 possessed

excellent properties (Table 2.1) (Jones and Clare, 2012) in terms of thermal, mechanical, physical and chemical properties.

Table 2.1: Properties of bioactive glasses. Adapted from Jones and Clare (2012).

Property	Value
Density	2.7
Network connectivity	2.12
Glass transition temperature	538 °C
Onset of crystallization	677 °C
Refractive index	1.59
Tensile strength	42 MPa
Young's modulus (stiffness)	35 MPa
Shear modulus	30.7 GPa
Fracture toughness	0.6 MPa m ^{1/2}
Vickers hardness	5.75 GPa

However, BG 45S5 had poor performance for mechanical properties (Vyas et al., 2015) which had lower values in flexural strength, microhardness and compressive strength (Table 2.2). Hence, other materials such as cobalt oxide and nickel oxide are incorporated within BG to improve its mechanical properties (Vyas et al., 2015; Vyas et al., 2016).

Table 2.2: Flexural strength, microhardness, compressive strength and density of bioactive glasses. Adapted from Jones and Clare (2012); Vyas, et al. (2015); Vyas et al. (2016).

Bioactive glass	45S5	NiO-1, NiO-2, NiO-3 and NiO-4	CoO-1, CoO-2, CoO-3 and CoO-4
Density	2.7	2.82 – 2.97	2.81 – 2.87
Compressive strength (MPa)	68.82	76.92 – 82.13	76.72 – 82.13
Flexural strength (Mpa)	43.48	55.15 – 66.58	56.25 – 65.78
Microhardness (GPa)	5.35	5.48 – 5.99	5.78 – 5.89

The network connectivity (N_c) is defined as the average number of the bridging oxygen atoms bounded to a network forming cation, where a BO (bridging oxygen) atom is defined as an oxygen atom which is chemically bound to two network polyhedral which is shown in equation 2.1 (Christie et al., 2016; Hill and Brauer, 2011).

$$\text{Network connectivity} = 2 + \frac{\text{BO} - \text{NBO}}{\text{G}} \quad (2.1)$$

Where,

BO = number of bridging oxygens

NBO = number of non-bridging oxygens

G = total number of glass-forming units

The non-bridging oxygen (NBO) was the oxygen atom that does not connect with the two networks polyhedral. Network connectivity (N_c) has been used successfully to predict the bioactivity of the bioactive glass. BG with N_c of 2.6 is bioactive but N_c more than 3.0 are likely to be inactive (Christie et al., 2016). Thus, network connectivity (N_c) was used to determine the ability of the bioactive glass to form apatite (Hill and Brauer, 2011). Network connectivity (N_c) of the BG depends on the composition of the BG since the presence of the network modifier cations may break the T–O–T bonds (where T is a network former, phosphorus in these glasses) (Christie et al., 2016).

Network connectivity of the BG can be modified by increasing or reducing the network modifier cations such as calcium and sodium for the BG composition. Lowering the BG network connectivity allows the BG to degrade easily and thus,

increasing its bioactivity (Christie et al., 2016). Moreover, structural, chemical, mechanical, bioactivity and the biological response of the BG can be determined by calculating the network connectivity (Arepalli et al., 2016). Lowering the Nc value of the BG results in better performance of the BG for cell compatibility and significant cell growth. Thus, the biocompatibility of the bioactive glass towards cell can also be determined by the network connectivity values. When increasing the composition of network modifiers, network connectivity of the bioactive glass tends to decrease leading to increased bioactivity properties (Arepalli et al., 2016).

Biocompatibility towards cell culture studies showed that concentration of BG powders by modulating the powder to liquid ratio plays an important role even though bioactive glass had their own values of network connectivity. Arepalli et. al, (2016) showed that all BG compositions were compatible with cells by using lower BG powder to liquid ratio (5 mg/ml). However, at higher BG powder to liquid ratio (10, 25, 50, 100, 250 and 500 mg/ml) of all BG compositions resulted in decreased cell viability after 24 hours. Hence, the ionic dissolution from the bioactive glass plays an important role in cell culture studies (Arepalli et al., 2016). Ionic dissolution products from the BG produced biological responses and usually resulted in their biological performance (Figure 2.1). Many researches have been conducted to understand the ionic dissolution products from the inorganic materials incorporated with different composition of BG and improving the biological performance (Hoppe et al., 2011).

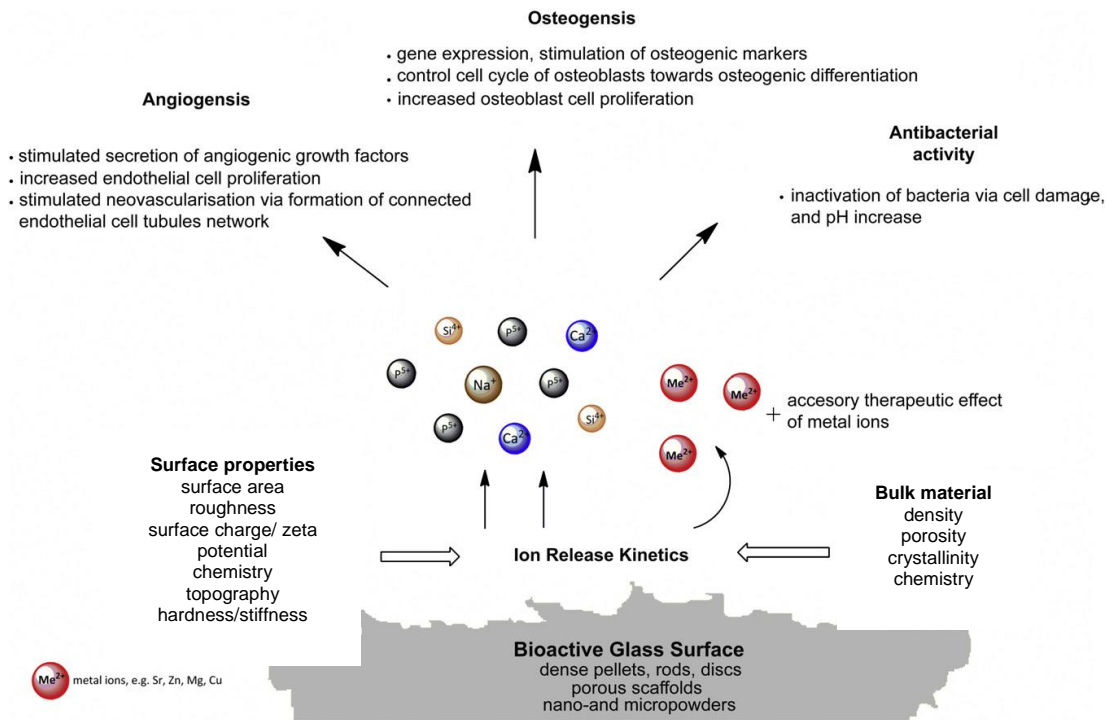


Figure 2.1: The biological responses to ionic dissolution products of bioactive glasses. Adapted from Hoppe et al., (2011).

Figure 2.2 shows different methods of investigating the biological response of BG using different BG size (small, large) and shape (pellets, rods, disc and scaffolds) fabricated from different methods (Hoppe et al., 2011). Direct method (Figure 2.2) involved preparing BG in scaffolds form (Chen and Thouas, 2011) by seeding the cells directly on the scaffolds itself. Indirect method (Figure 2.2) usually involved BG prepared in powder form (Silver et al., 2001) by treating the cells with extracts containing ionic dissolution products from BG powders. Thus, ionic dissolution products can affect biological performance of cells.

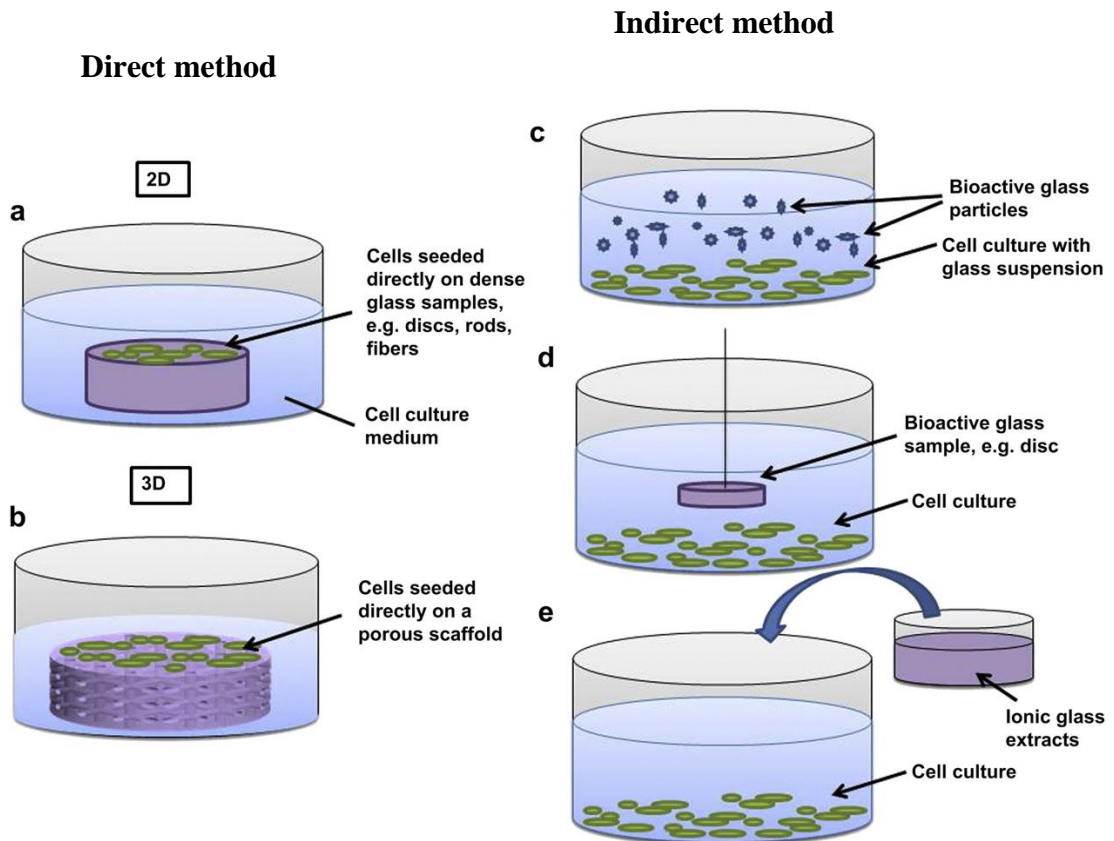


Figure 2.2: Methods for analysing the cellular response to degradable biomaterials. Adapted from Hoppe et al., (2011).

2.2.2 Synthesis of bioactive glass

Briefly, there are three processing methods commonly used to fabricate BG powders. BG can be synthesised by melt quench, sol-gel and also melt anneal routes. Each route requires different temperature, processing method and time needed that may affect the structure of the bioactive glass.

2.2.2(a) Melt quench route

Fabrication of BG *via* melt quench route requires high melting temperature. All of the raw materials involved were melted together in a crucible followed by rapid quench in distilled water. Various melting temperatures can be used for this route including 1370 °C until 1475 °C (Elgayar et al., 2005), 1380 °C (Zarifah et al., 2015), 1390 °C (O'Donnell et al., 2008a), 1400 °C (Ibrahim et al., 2017a) and up to 1500 °C (Sharma et al., 2016). It was previously shown that BG can be melted at temperature less than 1400 °C with melting temperature of BG 45S5 at 1377 °C based on DSC/TGA results (Ibrahim et al., 2017a).

However, the composition of BG itself may affect the BG melting temperature. O'Donnell et al., (2008a) proved that BG glass transition temperature decreased with increasing phosphate. Thus, each BG composition plays significant role in BG fabrication especially sodium which can reduce the melting temperature of BG (Wallace et al., 1999) due to disruption of BG structure. Furthermore, all of the bioactive glasses fabricated *via* melt quench route were in amorphous state even though its compositions were varied in mole percentages (Ibrahim et al., 2017b). BG fabricated *via* melt quench route can be produced in high volume within a short time with ease in obtaining the BG powders.

It had been reported that melt quench route is a suitable alternative to produce tougher materials, controlled dissolution rates and also bioactivity (Sepulveda et al., 2001). However, particle size of BG *via* melt quench route is larger compared to sol-gel which can affect the bioactivity of BG itself (Sepulveda et al., 2001). It is proven that BG 58S with composition of SiO₂ (60 mol.%), CaO (36 mol.%) and P₂O₅ (4 mol.%) as shown in Table 2.3 which had higher surface area with low particle size

released more calcium and silicon ions compared to melt derived BG 45S5 (Gong et al., 2014). Thus, ionic release of BG affects the differentiation, proliferation rate and mineralisation of cells due to different BG particle size. Hence, roughness and surface area of BG can be altered depending on the grinding process during fabrication (Sepulveda et al., 2002). Different grinding periods and media are able to change the range of the particle size obtained.

2.2.2(b) Sol-gel route

BG can also be fabricated through sol-gel route that affect the structure of the glass (Chen et al., 2008). Raw materials used for sol-gel route include tetraethoxysilane (TEOS, $\text{Si}(\text{OC}_2\text{H}_5)_4$), calcium nitrate tetra-hydrate ($\text{Ca}(\text{NO}_3)_2 \cdot 4\text{H}_2\text{O}$), sodium nitrate (NaNO_3) and also triethylphosphate (TEP, $\text{OP}(\text{OC}_2\text{H}_5)_3$). These materials were added into the aqueous solution of nitric acid (HNO_3) and subjected to stirring at room temperature for an hour. In order to form bioactive glass in gel form, the final solutions are kept at ambient temperature for 10 days to allow hydrolysis and polycondensation reactions to takes place. Then, the gel are aged between 60 °C until 120 °C for 7 days followed by thermal treatment for 20 hours at 700 °C (Dziadek et al., 2016).

The phosphate phases and crystalline silicate were present in the structure of BG synthesised *via* sol-gel route (Chen et al., 2008). Sol-gel route tend to produce lesser amount of BG in several days even though the process utilise temperature less than 1000 °C. BG fabricated *via* sol-gel route exhibits more polymerised silicon oxygen network compared to melt quench route as shown in FTIR results (Dziadek et al., 2016). Polymerised silicon oxygen network occurs in sol-gel route due to

stabilisation temperature for the gels, phase separation that can occur at sintering temperature and also presence of crystalline phases.

Thus, temperature treatment of the gels enhances the incorporation of network modifier which is calcium and sodium into the silicate network and leads to depolymerisation (Dziadek et al., 2016). Furthermore, BG *via* sol-gel route exhibit higher dissolution rates compared to melt quench BG, which tend to increase the rate of HA formation (Sepulveda et al., 2002). However, sol-gel route is very sensitive and require certain conditions such as pH, ratio and types of reactants, atmospheric conditions and temperature (Rezabeigi et al., 2014). Thus, steps in sol-gel route need to be properly controlled and monitor to obtain final product.

2.2.2(c) Melt anneal route

BG can also be synthesised *via* melt anneal route (Arepalli et al., 2016). Melt anneal route is adopted for obtaining BG with enhanced mechanical properties (Srivastava and Pyare, 2012). Batches of BG with fixed composition of CaO (24.50 wt.%), Na₂O (24.50 wt.%) and P₂O₅ (6.00 wt.%) while different compositions of SiO₂ (45.00, 44.00, 43.00, 42.00 and 41.00 wt.%) and CuO (1.00, 2.00, 3.00 and 4.00 wt.%) is melted in a platinum crucible at high temperature (1300 to 1500 °C) followed by pouring the molten glass on aluminium sheet or quenched in water. Then, the glass melts or frits that have been crushed were re-melted again followed by annealed for an hour and cooled to room temperature. The BG is melted again to ensure the homogeneity of the BG (Srivastava and Pyare, 2012) before anneal process begin.

Furthermore, heat treated samples is able to exhibit micro-structural changes in phase composition that changes the reactivity for the surface of BG upon immersion in SBF (Satyanarayana et al., 2017). It can be seen that chemical durability, micro hardness,

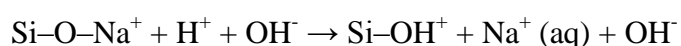
flexural strength and density of BG increased with increasing copper oxide content (Srivastava and Pyare, 2012). However, higher copper oxide compositions in BG resulted in lower crystallisation temperature and reduce glass nucleation. Thus, bioactivity of the BG tends to decrease due to decreased in crystallisation temperature of BG (Srivastava and Pyare, 2012).

2.2.3 Hydroxyl carbonate apatite (HCA) mechanism

Hydroxyl carbonate apatite (HCA) is formed on the BG surface upon immersion in simulated body fluid (SBF) after a certain period of time (Bellucci et al., 2011). Hydroxyl carbonate apatite (HCA) has a similar mineral constituent to the bone. Furthermore, commercialised BG 45S5 regenerates bone better than the commercialised hydroxyapatite (HA) (De Caluwé et al., 2016). The HCA mechanism involved 11 reactions sequence on the surface of the BG implant, as described by Hench (2006).

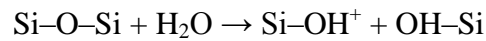
The first five sequences (Stage 1 until Stage 5) lead to formation of hydroxyl carbonate apatite (HCA) layer on the glass surface (Hench, 1998). After that, the sequences of reactions (Stage 6 until Stage 11) involve the effect of the ionic dissolution products that is released from the bioactive glass. The mechanism of HCA layer formation is shown in the following stages below:

Stage 1: Rapid cation exchange of Na^+ and/or Ca^{2+} with H^+ from solution, creating silanol bonds (Si-OH) on the glass surface.



The pH of the solution raises and a silica-rich (cation-depleted) region forms near the glass surface. Phosphate is also lost from the glass if present in the composition.

Stage 2: Soluble silica is lost in the form of $\text{Si}(\text{OH})_4$ to the solution due to Si-O-Si breaking bonds, leaving more Si-OH (silanols) at the glass-solution interface.



Stage 3: Condensation and repolymerisation of the Si-OH groups leaving the silica-rich layer on the glass surface.

Stage 4: Migration of Ca^{2+} and PO_4^{3-} groups to the glass surface through the silica-rich layer followed by formation of rich film in amorphous $\text{CaO-P}_2\text{O}_5$ rich film on top of the silica-rich layer.

Stage 5: The $\text{CaO-P}_2\text{O}_5$ rich film crystallises by incorporating OH^- and CO_3^{2-} anions from the solution followed by formation of hydroxyl carbonate apatite (HCA).

Stage 6: Adsorption of biological moieties in HCA layer.

Stage 7: Action of macrophages.

Stage 8: Osteoblast stem cells attachment.

Stage 9: Differentiation and proliferation of osteoblasts.

Stage 10: Generation of matrix.

Stage 11: Crystallisation of matrix and growth of bone.

The released ionic dissolution products (Si, Ca, Na and P) from the BG triggers intracellular and extracellular responses (Xynos et al., 2000). Effect from the ionic dissolution products are dose-dependent and response for each ions from the BG depends on the type of cells (Groh et al., 2014; Houreh et al., 2017; Liu et al., 2016a; Silva et al., 2017). The ability for bone bonding of BG is shown in the Figure 2.3 (Hench, 2006).

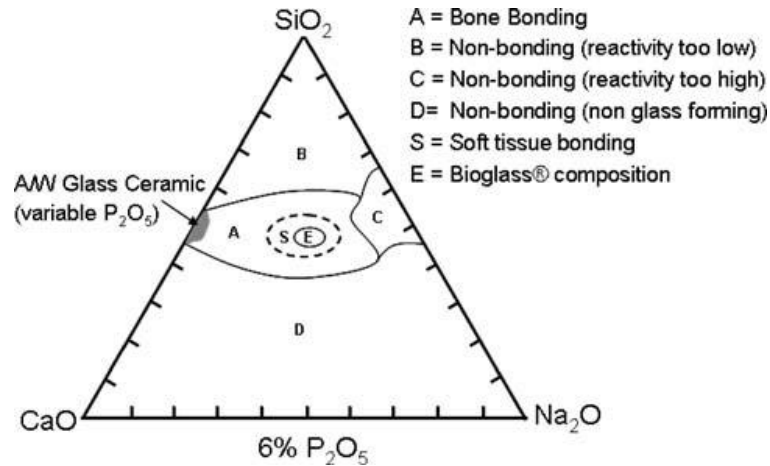


Figure 2.3: Compositional diagrams for bone-bonding in weight percentage. Adapted from Hench (2006).

BG compositional diagram shows different amount of SiO_2 , CaO and Na_2O with fixed amount of P_2O_5 in weight percentages (Figure 2.3). Moreover, BG 45S5 (region E) has the highest level of bioactivity, properties of bone bonding and also soft tissue bonding which is situated in the middle of the compositional diagram.

2.3 Modification in properties and composition of bioactive glass

The 45S5 Bioglass[®] has become one of the bioactive materials which can be used especially in dentistry. Thus, until now researchers investigate the original properties of BG 45S5 followed by modifying the original BG 45S5 composition (Dziadek et al., 2016) and also adding other elements such as strontium, fluoride and nickel oxide for better purposes (Arepalli et al., 2016; De Caluwé et al., 2016; Vyas et al., 2016) as shown in Table 2.3.

Table 2.3: Modification in bioactive glass composition based on standard 45S5 Bioglass®.

Name of the bioactive glass	Composition	References
BG 1, BG 2 and BG 3	- Fixed amount of SiO ₂ (60 mol.%). - Various amount of Na ₂ O (36, 32 and 28 mol.%) and and P ₂ O ₅ (4, 8 and 12 mol.%).	Houreh et al., 2017
A2	- SiO ₂ (40.0 mol.%), CaO (54.0 mol.%) and P ₂ O ₅ (6.0 mol.%) with network connectivity value (2.20).	Dziadek et al., 2016
Series I (ICSW2, ICSW3, ICSW4 and ICSW5)	- Various amount of SiO ₂ (47.84, 44.47, 40.96 and 37.28 mol.%), Na ₂ O (26.67, 27.26, 27.87 and 28.52 mol.%), CaO (23.33, 23.85, 24.39 and 24.95 mol.%) and P ₂ O ₅ (2.16, 4.42, 6.78 and 9.25 mol.%). - All compositions have different network connectivity values (2.18, 2.30, 2.44 and 2.62).	O'Donnell et al., 2008a
Series I (ICSW1, ICSW6, ICSW7, ICSW8, ICSW9 and ICSW10)	- Various amount of SiO ₂ (48.98, 47.07, 43.66, 40.71 and 38.14 mol.%), Na ₂ O (26.10, 26.67, 27.19, 28.12, 28.91 and 29.62 mol.%), CaO (23.33, 23.78, 24.60, 25.31 and 25.91 mol.%) and P ₂ O ₅ (1.02, 1.95, 3.62, 5.07 and 6.33 mol.%). - All compositions have same network connectivity value (2.08).	O'Donnell et al., 2008b
58S	- SiO ₂ (58.00 wt.%), CaO (33.00 mol.%) and P ₂ O ₅ (9.00 mol.%).	Chen et al., 2008
77S	- SiO ₂ (77.00 wt.%), CaO (14.00 mol.%) and P ₂ O ₅ (9.00 mol.%).	
Series B (ICIE6, ICIE7, ICIE8, and ICIE9)	- Fixed amount of Na ₂ O (13.19 mol.%) and P ₂ O ₅ (1.07 mol.%). - Various amount of SiO ₂ (48.46, 53.46, 56.46 and 61.00 mol.%) and CaO (37.27, 33.27, 30.27 and 25.27 mol.%). - All compositions have different network connectivity values (1.96, 2.29, 2.47 and 2.74).	Elgayar et al., 2005
Series C (ICIE10, ICIE11, ICIE12, ICIE13 and ICIE14)	- Fixed amount of K ₂ O (13.19 mol.%) and P ₂ O ₅ (1.07 mol.%). - Various amount of SiO ₂ (48.46, 49.46, 53.46, 56.46 and 61.00 mol.%) and CaO (37.27, 36.27, 33.27, 30.27 and 25.17 mol.%). - All compositions have different network connectivity values (1.96, 2.04, 2.29, 2.47 and 2.74).	

Table 2.3: Modification in bioactive glass composition based on standard 45S5 Bioglass[®] (continued).

Name of the bioactive glass	Composition	References
Series D (ICIE15, ICIE16, ICIE17, ICIE18 and ICIE19)	<ul style="list-style-type: none"> - Fixed amount of Na₂O (6.60 mol.%), K₂O (6.60 mol.%) and P₂O₅ (1.07 mol.%). - Various amount of SiO₂ (48.46, 49.46, 53.46, 56.46 and 61.00 mol.%) and CaO (37.27, 36.27, 33.27, 30.27 and 25.17 mol.%). - All compositions have different network connectivity values (1.96, 2.04, 2.29, 2.47 and 2.74). 	Elgayar et al., 2005
Li25, Li50, Li75 and Li100	<ul style="list-style-type: none"> - Fixed amount of SiO₂ (46.1 mol.%), CaO (26.9 mol.%) and P₂O₅ (2.6 mol.%). - Various amount of Na₂O (18.3, 12.2, 6.1 and 0 mol.%). - Addition of Li₂O (6.1, 12.2, 18.3 and 24.4 mol.%) 	Silva et al., 2017
Zn0, Zn1, Zn2 and Zn3.	<ul style="list-style-type: none"> - Various amount of SiO₂ (38.5, 37.0, 35.7 and 34.3 mol.%), Na₂O (26.2, 26.5, 26.7 and 27.0 mol.%), CaO (29.0, 29.2, 29.4 and 29.6 mol.%) and P₂O₅ (6.3, 6.2 and 6.1 mol.%). - Addition of ZnO (0, 1.0, 2.0 and 3.0 mol.%) - Network connectivity value (2.10). 	Huang et al., 2017
NiO-1, NiO-2, NiO-3 and NiO-4	<ul style="list-style-type: none"> - Various amount of SiO₂ (45.64, 45.20, 44.71 and 44.25 mol.%), Na₂O (24.41, 24.44, 24.46 and 24.49 mol.%), CaO (26.94, 26.96, 26.98 and 27.01 mol.%) and P₂O₅ (2.60 and 2.61 mol.%). - Addition of NiO (0.41, 0.82, 1.23 and 1.65 mol.%). 	Vyas et al., 2016
Sr-0, Sr-1, Sr-2, Sr-3 and Sr-4	<ul style="list-style-type: none"> - Fixed amount of Na₂O (24.40 mol.%) and P₂O₅ (2.60 mol.%). - Various amount of SiO₂ (46.10, 45.10, 44.10 and 43.10 mol.%), and CaO (26.90 and 24.22 mol.%). - Addition of SrO (1.00, 2.00 and 3.00 mol.%). - All compositions have different network connectivity values (1.84, 1.94, 2.03 and 2.11). 	Arepalli et al., 2016
45S5F	<ul style="list-style-type: none"> - SiO₂ (47.71 mol.%), Na₂O (25.19 mol.%), CaO (14.20 mol.%) and P₂O₅ (2.69 mol.%). - Addition of CaF₂ (10.20 mol.%). - Network connectivity value (2.68). 	De Caluwé et al., 2016

Table 2.3: Modification in bioactive glass composition based on standard 45S5 Bioglass® (continued).

Name of the bioactive glass	Composition	References
CF9	<ul style="list-style-type: none"> - SiO₂ (34.60 mol.%), CaO (50.38 mol.%) and P₂O₅ (5.74 mol.%). - Addition of CaF₂ (9.28 mol.%). - Network connectivity value (2.08). 	De Caluwé et al., 2016
CoO-1, CoO-2, CoO-3 and CoO-4	<ul style="list-style-type: none"> - Fixed amount of Na₂O (24.50 wt.%), CaO (24.50 wt.%) and P₂O₅ (6.0 wt.%). - Various amount of SiO₂ (44.50, 44.00, 43.50 and 43.00 wt.%). - Addition of CoO (0.50, 1.00, 1.50 and 2.00 wt.%). 	Vyas et al., 2015
C1, C2, C3 and C4	<ul style="list-style-type: none"> - Fixed amount of Na₂O (24.50 wt.%), CaO (24.50 wt.%) and P₂O₅ (6.0 wt.%). - Various amount of SiO₂ (44.00, 43.00, 42.00 and 41.00 wt.%). - Addition of CuO (1.00, 2.00, 3.00 and 4.00 wt.%). 	Srivastava and Pyare, 2012
BG_Na	<ul style="list-style-type: none"> - SiO₂ (48.7 mol.%), Na₂O (33 mol.%), CaO (15.6 mol.%) and P₂O₅ (2.6 mol.%). 	Bellucci et al., 2011
BG_Ca	<ul style="list-style-type: none"> - SiO₂ (47.2 mol.%), Na₂O (4.6 mol.%), CaO (45.6 mol.%) and P₂O₅ (2.6 mol.%). 	
BioK	<ul style="list-style-type: none"> - SiO₂ (46.1 mol.%), K₂O (24.4 mol.%), CaO (26.9 mol.%) and P₂O₅ (2.6 mol.%). 	
Mg Series ICIE1 – (25 Mg, 50 Mg, 75 Mg and 100 Mg)	<ul style="list-style-type: none"> - Fix amount of SiO₂ (49.46 mol.%), Na₂O (26.38 mol.%) and P₂O₅ (1.07 mol.%). - Various amount of CaO (23.08, 17.31, 11.54, 5.77 and 0 mol.%) - Addition of MgO (0, 5.77, 11.54, 17.31 and 23.08 mol.%). - Network connectivity value (2.13). 	Hill and Brauer, 2011
P Series I ICSW1, ICIE1, ICSW2, ICSW3, ICSW5 and ICSW4	<ul style="list-style-type: none"> - Various amount of SiO₂ (51.06, 49.46, 47.84, 44.47, 40.96 and 37.28 mol.%), Na₂O (26.10, 26.38, 26.67, 27.26, 27.87 and 28.52 mol.%), CaO (22.84, 23.08, 23.33, 23.85, 24.39 and 24.95 mol.%) and P₂O₅ (0, 1.07, 2.16, 4.42, 6.78 and 9.25 mol.%). - All composition have different network connectivity values (2.08, 21.3, 2.18, 2.30, 2.44 and 2.62). 	